Manipulation of peripheral neural feedback loops alters human corticomuscular coherence

C. Nicholas Riddle[1] and Stuart N. Baker[2]

[1] *Department of Anatomy, University of Cambridge, Cambridge CB2 3DY, UK*
[2] *School of Clinical Medical Sciences, University of Newcastle, Sir James Spence Institute, Royal Victoria Infirmary, Queen Victoria Road, Newcastle upon Tyne NE1 4LP, UK*

Sensorimotor EEG shows ∼20 Hz coherence with contralateral EMG. This could involve efferent and/or afferent components of the sensorimotor loop. We investigated the pathways responsible for coherence genesis by manipulating nervous conduction delays using cooling. Coherence between left sensorimotor EEG and right EMG from three hand and two forearm muscles was assessed in healthy subjects during the hold phase of a precision grip task. The right arm was then cooled to 10°C for ∼90 min, increasing peripheral motor conduction time (PMCT) by ∼35% (assessed by F-wave latency). EEG and EMG recordings were repeated, and coherence recalculated. Control recordings revealed a heterogeneous subject population. In 6/15 subjects (Group A), the corticomuscular coherence phase increased linearly with frequency, as expected if oscillations were propagated along efferent pathways from cortex to muscle. The mean corticomuscular conduction delay for intrinsic hand muscles calculated from the phase–frequency regression slope was 10.4 ms; this is smaller than the delay expected for conduction over fast corticospinal pathways. In 8/15 subjects (Group B), the phase showed no dependence with frequency. One subject showed both Group A and Group B patterns over different frequency ranges. Following cooling, averaged corticomuscular coherence was decreased in Group A subjects, but unchanged for Group B, even though both groups showed comparable slowing of nervous conduction. The delay calculated from the slope of the phase–frequency regression was increased following cooling. However, the size of this increase was around twice the rise in PMCT measured using the F-wave (regression slope 2.33, 95% confidence limits 1.30–3.36). Both afferent and efferent peripheral nerves will be slowed by similar amounts following cooling. The change in delay calculated from the coherence phase therefore better matches the rise in total sensorimotor feedback loop time caused by cooling, rather than just the change in the efferent limb. A model of corticomuscular coherence which assumes that only efferent pathways contribute cannot be reconciled to these results. The data rather suggest that afferent feedback pathways may also play a role in the genesis of corticomuscular coherence.

(Resubmitted 1 May 2005; accepted after revision 22 May 2005; first published online 26 May 2005)
Corresponding author S.N. Baker: School of Clinical Medical Sciences, University of Newcastle, Sir James Spence Institute, Royal Victoria Infirmary, Queen Victoria Road, Newcastle upon Tyne NE1 4LP, UK.
Email: stuart.baker @ncl.ac.uk

There has been much recent interest in motor cortical oscillations, where rhythms at ∼10 Hz and ∼15–30 Hz occur in both animals and humans (Salmelin & Hari, 1994; Murthy & Fetz, 1996; Stancak & Pfurtscheller, 1996; Baker *et al.* 1997; Salenius *et al.* 1997; Donoghue *et al.* 1998; Halliday *et al.* 1998; Brown *et al.* 1998; Mima & Hallett, 1999; Kilner *et al.* 2000). These oscillations are abolished during movement, and are greatest during periods of steady contraction (Pfurtscheller & Neuper, 1992; Stancak & Pfurtscheller, 1996; Pfurtscheller *et al.* 1996; Baker *et al.* 1997; Kilner *et al.* 1999). Similar oscillations are observed in the EMG of contracting muscles; those around 20 Hz show coherence with simultaneously recorded cortical activity (Conway *et al.* 1995; Baker *et al.* 1997; Salenius *et al.* 1997; Hari & Salenius, 1999; Kilner *et al.* 1999). This corticomuscular coherence has also been shown to be task dependent (Baker *et al.* 1997; Kilner *et al.* 2000). Despite much effort, it remains obscure what function these oscillations might play.

Corticomuscular coherence is commonly regarded as an efferent phenomenon, whereby oscillations are propagated from their cortical source to spinal motoneurones, probably via the corticospinal tract (McAuley *et al.* 1997; Salenius *et al.* 1997; Hari & Salenius, 1999; Gross *et al.*

 DOI: 10.1113/jphysiol.2005.089607

2000). However, the situation may be more complex. Firstly, although both ∼10 Hz and ∼20 Hz frequency bands are propagated down the corticospinal tract (Baker *et al.* 2003), only ∼20 Hz coherence is normally seen (Baker *et al.* 1997; Kilner *et al.* 1999, 2000). Further complexity comes from studies of the coherence phase–frequency relationship, an important parameter which can constrain the range of possible network topographies underlying the phenomenon. Coherence generation solely by efferent propagation would imply a linearly increasing coherence phase–frequency relationship, indicating a constant delay (Rosenberg *et al.* 1989). Some authors have observed this, with a calculated delay broadly consistent with corticospinal and peripheral efferent nerve conduction. By contrast, other reports show a constant coherence phase across a range of frequencies (Halliday *et al.* 1998; Marsden *et al.* 1999).

Afferent feedback could also contribute to coherence. Motor cortical cells receive strong peripheral input (Lemon, 1979). Muscle spindle receptors, amongst others, are exquisitely sensitive to small perturbations (Matthews, 1972), and would thus provide a considerable afferent input back to the cortex at tremor frequencies which include 20 Hz (Stiles & Randall, 1967; McAuley *et al.* 1997; Vaillancourt & Newell, 2000). If a substantive afferent contribution does exist, its recognition could stimulate a paradigm shift in understanding the function of coherent oscillations in the motor cortex. Rather than assuming a purely motor role, we would be free to explore a wider range of possible functions involving sensorimotor integration.

In this study, we investigated the generation of corticomuscular coherence using arm cooling to slow (but not abolish) peripheral nervous conduction in both afferent and efferent nerves. Our detailed quantitative measurements could not be reconciled with a purely efferent model of coherence generation. Instead, they strongly suggest that corticomuscular coherence results from a complex interaction of the motor command with sensory feedback.

Methods

Experiments were performed on 15 young, healthy volunteer subjects (10 male), all right handed by self-report. Subjects gave informed written consent in accordance with the Declaration of Helsinki and all procedures were approved by the local Human Biology Research Ethics Committee.

Recordings

Bipolar EMG recordings were made from five muscles in the right hand and forearm using adhesive surface electrodes (Biotrace 0713C, MSB Ltd, Marlbrough, UK) placed over the muscle belly. The muscles recorded were first dorsal interosseous (1DI), abductor pollicis brevis (AbPB), abductor digiti minimi (AbDM), flexor digitorum superficialis (FDS) and extensor digitorum communis (EDC). The first three comprise the intrinsic muscles of the hand, while FDS and EDC are forearm muscles. Differential EEG was recorded from the left sensorimotor cortex using two adhesive scalp electrodes (Neuroline 720 00-S, Medicotest, St Ives, UK), with the anterior electrode connected to the non-inverting input of the amplifier. The electrodes were positioned 30 mm lateral to the vertex, and 20 mm anterior and posterior to the interaural line, locations previously shown to be effective in recording sensorimotor EEG (Baker & Baker, 2003). Signals were amplified (EMG gain 100–5000; EEG gain 50 k) and band-pass filtered (EMG 30 Hz–2 kHz; EEG 3 Hz–2 kHz) before being digitized at 4273.5 Hz by a Power1401 interface (Cambridge Electronic Design Ltd, Cambridge, UK) connected to a PC running Spike2 software (Cambridge Electronic Design Ltd).

Behavioural task

Subjects performed a precision grip task identical to that used in our previous work ('AUX1' task of Kilner *et al.* 2000; Baker & Baker, 2003; Riddle *et al.* 2004). The manipulandum comprised two aluminium levers ($20 \times 80 \times 1.5$ mm) mounted on the shafts of computer-controlled torque motors, programmed to simulate an auxotonic (spring-like) load. At rest the levers lay 70 mm apart. Lever position was measured by two optical encoders (resolution 10160 counts/revolution) attached to the motor shafts.

Subjects were seated in front of a computer monitor, and gripped the levers between finger and thumb in a precision grip. They tracked two on-screen targets with cursors linked to finger movement. An initial force of 1 N was required to move the levers off their end-stops. The targets produced a hold–ramp–hold pattern, with the first hold requiring a rapid lever displacement of 12 mm from rest, at a force level of 1.3 N. After holding at this level for 3 s, the targets produced a 2 s ramp movement to reach the second hold, which lay 24 mm from rest at 1.6 N force. This hold lasted a further 3 s before the targets disappeared and subjects were required to release the levers.

Arm cooling

The right arm was cooled using water at 10°C. This temperature was chosen following Matthews (1989), as being well within the safe range. Lower temperatures are inadvisable since they risk inducing hypothermic conditions analogous to 'immersion foot' (Matthews, 1989). The system used water cooled to ∼4°C using crushed ice in a 50 l reservoir raised to a height of 3 m above floor level. The output from this reservoir flowed under

gravity through a valve whose position was set by a servo motor under computer control. This cold flow was mixed with room temperature water from a second elevated reservoir. The temperature of the mixture was determined by a platinum resistance thermometer (Farnell, Leeds, UK). A feedback algorithm used this temperature reading to adjust the cold outflow valve position, thereby altering the mixture water temperature to maintain a set point. This system was shown to be accurate to within 0.1°C, and could successfully maintain a mixture temperature of 10°C for the duration of the experiment. Two thin-walled rubber tubes were wrapped around the subject's arm from the axilla to the wrist, with care taken to ensure they were not too tight. The cooled water flowed through these tubes in parallel from proximal to distal before returning to a third reservoir at floor level. Water was recycled back into the system by an immersion pump.

A platinum resistance thermometer was mounted on the dorsum of the hand to measure skin temperature. Before the onset of cooling, a baseline temperature measurement was made. The skin temperature was maintained at this level ±0.5°C, using a heat lamp under negative feedback control. In this way we ensured that while the arm was cooled, the intrinsic muscles of the hand remained at a normal temperature.

In a pilot experiment, the subject reported minor motor impairment in his right hand following cooling. This recovered completely after three days and was attributed to water pressure being too high; Matthews (1989) reported a similar experience during his initial experiments. A restrictor was therefore applied to the system outflow in subsequent experiments, which reduced the water pressure flowing through the rubber tubing. No subsequent subjects reported adverse effects. At the onset of cooling, when the cold water first entered the rubber tubing, several subjects reported transient arm pain associated with the water temperature. However, in all cases this subsided after ∼30 s, with no further pain or discomfort reported.

F-wave assessment of motor conduction time

Two adhesive electrodes were placed over the right median nerve at the wrist, and connected to a constant current nerve stimulator (Digitimer DS7A, Digitimer Ltd, Welwyn Garden City, UK; cathode distal; 0.5 ms pulse width). The F-wave in AbPB was elicited using stimuli at 1 Hz, at an intensity supramaximal for generation of an M wave. An online assessment of the progress of cooling was obtained by measuring the earliest onset latency of around 50 F-wave responses. Off-line, the F-wave latency was determined as the 10th percentile of the latency distribution (Olivier *et al.* 2002). The peripheral motor conduction time (PMCT) is given by:

$$\mathrm{PMCT} = (M + F - 1)/2$$

where M is the latency of the direct M response, F is the latency of the F-wave, and the 1 ms term represents a correction for the delay in re-excitation of the motoneurone (Kimura, 1989). Accordingly, the size of the slowing in PMCT following cooling was estimated as half the sum of the increase in M and F wave latency.

Experimental protocol

At the start of the experiment, control data were taken for F-wave latency, and from 80 trials of the precision grip task.

The rubber tubing was then wrapped around the subject's right arm, and cooling commenced. F-wave latency was assessed every 10 min, and cooling continued until it rose by around 35%; this normally required approximately 90 min of cooling. Subjects then performed a second run of 80 trials of the precision grip task, while the arm was maintained cold. A final measurement of F-wave latency was taken, and the subject disconnected from the apparatus; the arm was allowed to warm up naturally. The radial pulse and finger nail capillary refill time were checked regularly throughout the experiment and were normal at all times.

Analysis

All data analysis was performed using custom-written MATLAB (Mathworks Inc.) routines. Analysis focused upon the second hold period of the precision grip task as corticomuscular coherence is greatest during this period (Kilner *et al.* 2000). Before further analysis, all signals were resampled to 5 kHz to facilitate subsequent noise removal. Some hand muscle EMGs in some subjects showed moderate levels of 50 Hz noise, due to the close proximity of the heat lamp. All channels were therefore first passed through an algorithm which removed noise components which were phase locked to the 50 Hz mains supply (this algorithm required a sampling rate which was a multiple of 50 Hz). Following this, EMGs were full wave rectified. EEG and EMG power spectra were computed, as was coherence between EEG and EMG – these analyses used two contiguous 1.28-s-long sections of data taken from the second hold period of each trial and a 6400-point long fast Fourier transform (Baker *et al.* 1997), yielding a frequency resolution of 0.78 Hz. Power spectra for EEG and EMG data were first normalized to the total power across all frequencies in that signal in the control recording. The spectra were then averaged across subjects in each group for EEG, and across subjects and muscles in each group for EMG and coherence. Significance limits for averaged coherence were calculated according to the method described in Evans & Baker (2003). Significant differences in coherence between cooled and control conditions were calculated using the method described

in Riddle *et al.* (2004). Phase spectra were calculated from the argument of the complex cross spectra; 95% confidence limits were determined on each phase estimate according to the formulae given by Rosenberg *et al.* (1989).

Results

Effects of cooling

Figure 1 illustrates a typical profile of F-wave changes for a single representative subject as the arm was slowly cooled over a period of ∼110 min. Median nerve stimulation elicited clear F-waves whose onset latency increased steadily throughout cooling (arrowheads, Fig. 1*A*). This is seen in Fig. 1*B* and *C*, which show the onset latencies for the population of F-waves at the start of cooling (Fig. 1*B*) and the end point (Fig. 1*C*). The 10th percentile of F-wave latency changed from 31.4 ms to 43.2 ms in this example, an increase of 37.6%. This increase occurred in a reasonably uniform fashion throughout the period of cooling (Fig. 1*D*). Similar profiles were observed for all other subjects, indicating the success of the cooling protocol in slowing nervous conduction. Evoked potentials from C7 spinal rootlets following median nerve stimulation at the wrist were additionally recorded in four subjects (data not shown), to provide a control for the F-wave measures. Onset latencies were seen to increase in a fashion comparable in magnitude to that of the F-waves following cooling, thus further corroborating the success of the protocol.

The cooling system was designed to cool the nerves of the forearm selectively without affecting the mechanical properties of the intrinsic muscles of the hand which they supply. To assess the success of this approach, we measured muscle twitch times in the hand and forearm muscles of two subjects, either by stimulating the 1DI muscle directly

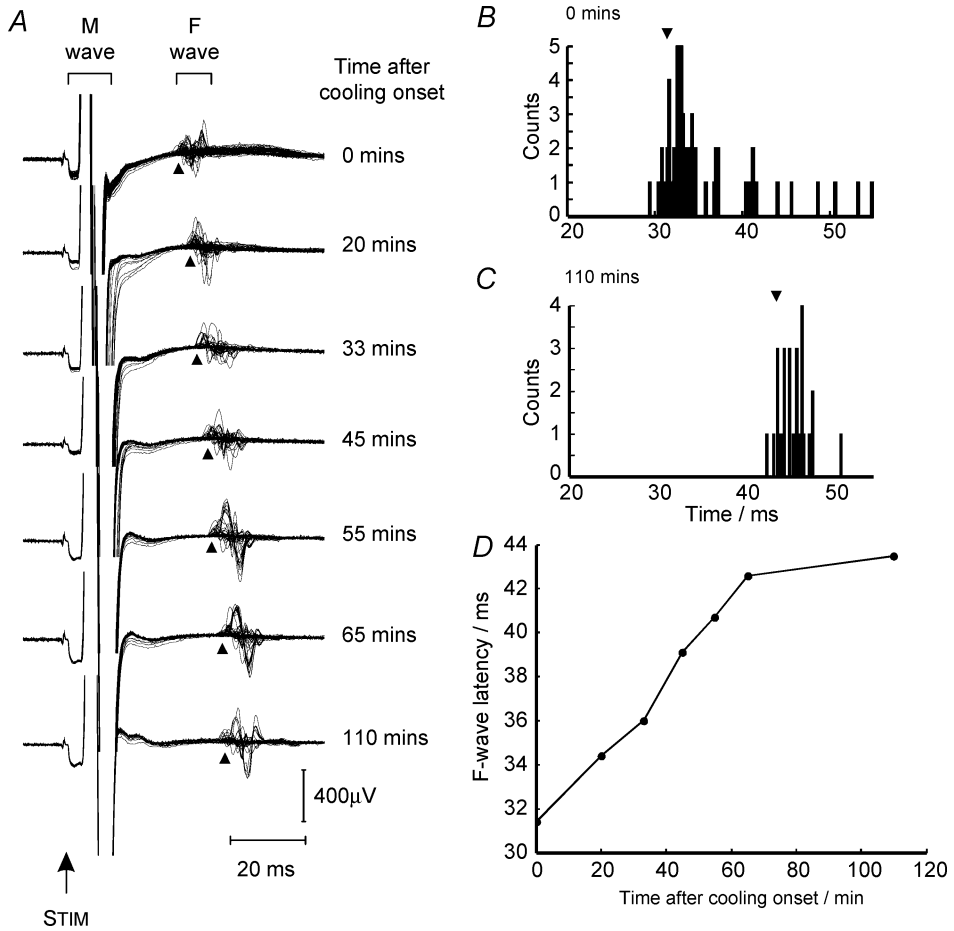

Figure 1. Change in F-wave latency during arm cooling in a single subject
A, F-waves elicited by stimulation of the median nerve at the wrist at different times after the onset of cooling. Each trace shows 30–40 superimposed sweeps. M-wave clipped for clarity. Arrowheads mark the 10th percentile F-wave onset latency. STIM, point of stimulus delivery. *B* and *C*, histograms of F-wave latency at the start (*B*) and end (*C*) of cooling. Arrowheads indicate the 10th percentile of the latency distribution. *D*, 10th percentile of F-wave latency plotted against time after cooling onset. Subject 2tt.

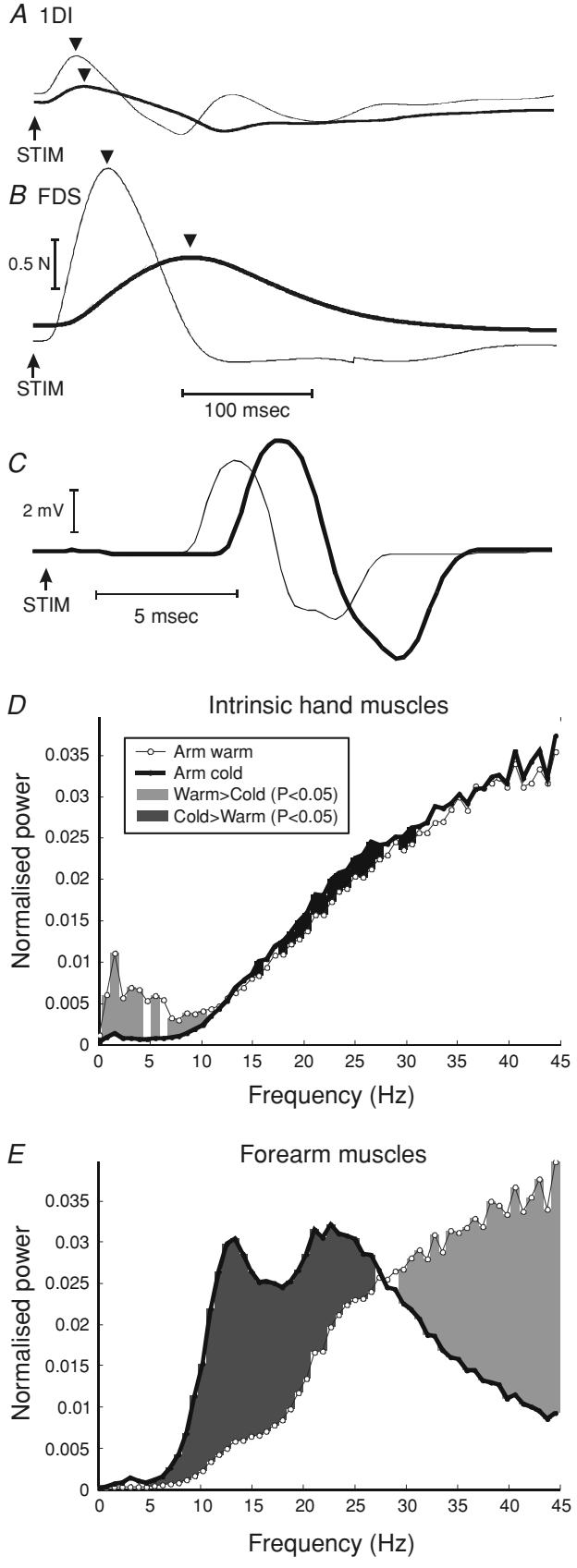

through the surface EMG electrodes, or by stimulating the median nerve at the cubital fossa which activated wrist and finger flexors. Subjects performed a gentle isometric contraction which pressed the finger against a strain gauge, either in abduction (for 1DI), or flexion. Figure 2*A* and *B* shows the averaged force records following stimulation of each muscle in one subject. While the twitch time of 1DI showed negligible change following cooling (35 ms before, 37 ms after cooling; arrowheads, Fig. 2*A*), it more than doubled for flexion (58 ms before, 125 ms after cooling; arrowheads, Fig. 2*B*). A similar result was seen in the second subject. It is clear that the mechanical properties of the forearm muscles were very significantly altered by the direct cooling they received. Although some alteration in motor unit responses was probably produced in the intrinsic hand muscles, it was considerably smaller. In the subject illustrated, the peak twitch amplitude was reduced in the recording following cooling for both 1DI and FDS. However, this was not consistent between subjects, and probably related to minor movements of the surface stimulating electrodes on the skin relative to the underlying nerve or muscle, which can substantially alter the amplitude of activation seen.

Figure 2*C* illustrates how the M-wave in AbPB was altered by the cooling protocol (same subject as illustrated in Fig. 1). In this subject, there was a small increase of 1.3 ms in the duration of the M-wave (measured from onset to the negative peak). This compared with a 6.5 ms increase in PMCT in this subject. Over the subject pool, M-wave durations were increased on average by 1.4 ms (range 0.4–2.5 ms). Thus while changes in the EMG of the intrinsic hand muscles did occur during cooling, they were minor compared to the changes in nervous conduction velocity.

Further verification of this finding was provided by examination of the power spectra of the unrectified EMG. The power of the unrectified EMG is largely dominated by the shape of the individual motor unit action potentials (MUAP). In a bipolar recording, the MUAP duration will depend on the speed of propagation of action potentials along the muscle fibres. Muscle cooling will slow muscle fibre conduction velocity, and hence prolong MUAP

Figure 2. Intrinsic hand muscles and forearm muscles were affected differently by cooling
A and *B*, average force produced by electrical stimulation of an intrinsic hand muscle (*A*, 1DI, direct stimulation over belly of muscle) and a forearm muscle (*B*, FDS, stimulation of median nerve at cubital fossa). Thin lines, control data; thick lines, after cooling. Arrowheads denote points of maximum force used for twitch time measurement. $n = 22$–39 stimuli. Subject 8cnr. *C*, M-wave duration increased only marginally following cooling. STIM, point of stimulus delivery to median nerve at the wrist. Thin lines, control data; thick lines, after cooling. Subject 2tt. *D* and *E*, power spectra of unrectified EMG from intrinsic hand muscles (*D*) and forearm muscles (*E*). Spectra are averaged across all muscles and subjects: $n = 45$ for intrinsic hand muscles and $n = 30$ for forearm muscles.

duration. This should lead to a shift of the unrectified EMG power spectra to lower frequencies. Figure 2*D* shows the unrectified EMG power spectra of the three intrinsic hand muscles averaged across all 15 subjects. There was a small but significant increase in EMG power in the 15.7–30.5 Hz range following cooling (dark grey bars, Fig. 2*D*). This probably represents slight lengthening of the MUAP durations, confirming that some slowing of myofibril conduction did occur in the intrinsic hand muscles, despite their isolation from direct cooling. There was also a significant decrease in power following cooling at low frequencies, probably as a result of the normalization implied by the calculation of relative power. By contrast, the forearm muscle unrectified EMG spectrum, averaged across all subjects, showed a very much larger shift towards the lower frequency range following cooling (Fig. 2*E*). The magnitude of this shift is almost certainly greater than Fig. 2*E* implies, since the EMG amplifiers used had a high-pass filter setting of 30 Hz and the power at lower frequencies will therefore have been much attenuated by the filter. These data suggest that muscle action potential propagation speed was considerably slowed in the forearm muscles following cooling, whereas in the intrinsic hand muscles the slowing was minor.

The data of Fig. 2 imply, using very different techniques, that our attempt to maintain the hand at its normal temperature during the experiment was reasonably, although not completely, successful. For the forearm muscles, cooling profoundly affected both the muscle mechanical and electrical properties and the conduction velocity of the nerves supplying them. By contrast, for the intrinsic hand muscles, although the nervous conduction was slowed, the direct effects on the muscles were smaller.

Phase of corticomuscular coherence

When the phase of corticomuscular coherence was calculated, it appeared that the subjects formed a non-homogenous population, with two predominant groups evident. In order to quantify this observation and thence construct objective groupings, we considered the control recording from each subject prior to cooling. For each subject, the phase was determined for frequencies where the coherence was significantly above zero. Phase measurements from the three intrinsic hand muscles were superimposed on a single plot, since the peripheral nervous conduction time for these muscles is likely to be similar, and this increased the number of phase estimates which could be used in the analysis. A regression line was then fitted to points in the frequency range of interest from 10 to 30 Hz; neither the slope nor the intercept of this line were constrained. The 95% confidence limits placed on the slope by the regression analysis were used to determine whether the slope was significantly different from zero.

Single-subject examples of the groups revealed by this analysis are illustrated in Fig. 3. The first group (Group A, Fig. 3*A* and 6/15 subjects) had a linearly increasing phase frequency relationship with a slope significantly different from zero. In all such cases, the slope was positive, indicating that the EEG led the EMG. By contrast, in the second group of subjects (Group B, Fig. 3*B* and 8/15 subjects) the phase–frequency plots were flat, with a regression slope of zero. Finally, one subject interestingly showed both patterns, with a zero slope phase–frequency relationship between 12.5 and 24.2 Hz, and a clear linear dependence between 27.4 and 37.5 Hz (Fig. 3*C*). This subject was therefore classified as in neither group.

Figure 3*D* shows a histogram of the slopes of the linear regression fits for all subjects. The slopes have been rescaled so that they can be interpreted as the delay between the EEG and EMG. The black bars indicate values which were significantly different from zero; for these subjects, the mean delay was 10.4 ms The distribution of slopes appeared bimodal, confirming that subjects did indeed fall into distinct groups. Accordingly, all further analysis was carried out separately for the different groups.

It should be emphasized that this grouping of subjects was based purely on the above analysis of differences in coherence phase. There was no significant difference between the groups in the slowing of PMCT following cooling (as assessed by the F-wave). The mean PMCT increase across all subjects was 35%.

Effects of cooling on corticomuscular coherence

Figure 4 shows examples of corticomuscular coherence for single subjects taken from each of the two groups, plus the anomalous subject who did not fit either grouping. For each subject, coherence was averaged separately across the three intrinsic hand muscles and the two forearm muscles, because of the differential effects of cooling upon these two muscle groups outlined above. Group A subjects showed a significant decrease in coherence (Fig. 4*A* and *B*). For the intrinsic muscles in the subject illustrated, 8/22 bins showed a significant decrease in coherence following cooling ($P < 0.05$, light grey bars, Fig. 4*A*) in the coherent band between 11.7 Hz and 28.1 Hz. By contrast, only 2/22 bins showed a significant increase ($P < 0.05$, dark grey bars, Fig. 4*A*). A similar pattern was observed for the forearm muscles, although the decrease in coherence following cooling was greater – the maximum decrease for the subject in Fig. 4*A* and *B* was from 0.082 to 0.019 (76.4%) at 24.2 Hz for the intrinsic muscles, and from 0.085 to 0.010 (87.8%) at 25.0 Hz for the forearm muscles.

Figure 4*C* and *D* shows the same analysis for a Group B subject. In contrast to the Group A population, these subjects showed little or no change in coherence following cooling. In the example shown here, neither the intrinsic (Fig. 4*C*) nor forearm (Fig. 4*D*) muscles showed any significant changes in coherence after cooling, apart from one significant decrease in the 45 Hz frequency bin.

For the single anomalous subject, a dual pattern was once again observed (Fig. 4*E* and *F*). For the intrinsic hand muscles in the lower frequency range (12.5–24.2 Hz), corresponding to the portion of the phase–frequency plot with zero slope similar to Group B subjects, coherence was unchanged after cooling apart from in two frequency bins where there was a significant increase (Fig. 4*E*). At higher frequencies, where phase increased linearly with frequency as in Group A subjects, coherence decreased significantly following cooling. A similar pattern was seen in the forearm muscles (Fig. 4*F*), although with a greater number of bins showing a significant decrease at higher frequencies than was evident in the intrinsic muscles (7 bins compared to 5; light grey bars, Fig. 4*E* and *F*).

Figures 5 and 6 illustrate data averaged across all subjects within each group for power and coherence before and after cooling. Figure 5 shows the EEG and EMG power. For each group, EEG power spectra showed characteristic peaks at ∼10 Hz and, for Groups A and B, at ∼20 Hz (Fig. 5*A*–*C*). For the single subject not in Group A or B, there was little evidence of a ∼20 Hz peak, but this was replaced with a strong ∼33 Hz component (Fig. 5*C*). These peaks represent the dominant oscillatory activities present in the motor cortical region underlying the electrodes. The higher-frequency peak seen for this subject probably reflects natural variation (see Kilner *et al.* 1999). The low-frequency (∼3 Hz) peaks seen in each spectrum probably result artefactually from the 3 Hz high-pass filter setting of the amplifier. Following cooling, Group A and the anomalous subject showed no changes in the amplitude or peak frequencies of the EEG, while Group B showed a very small but significant increase in power amplitude in four bins between 17.9 Hz and 24.2 Hz (dark grey bars, Fig. 5*B*).

Power spectra of the full-wave-rectified EMG for the three groups are shown in Fig. 5*D*–*I*, averaged separately across the intrinsic hand muscles and forearm muscles. In all groups, the changes in intrinsic muscle spectral power following cooling which reached significance were small (Fig. 5*D* and *E*). By contrast, much larger and

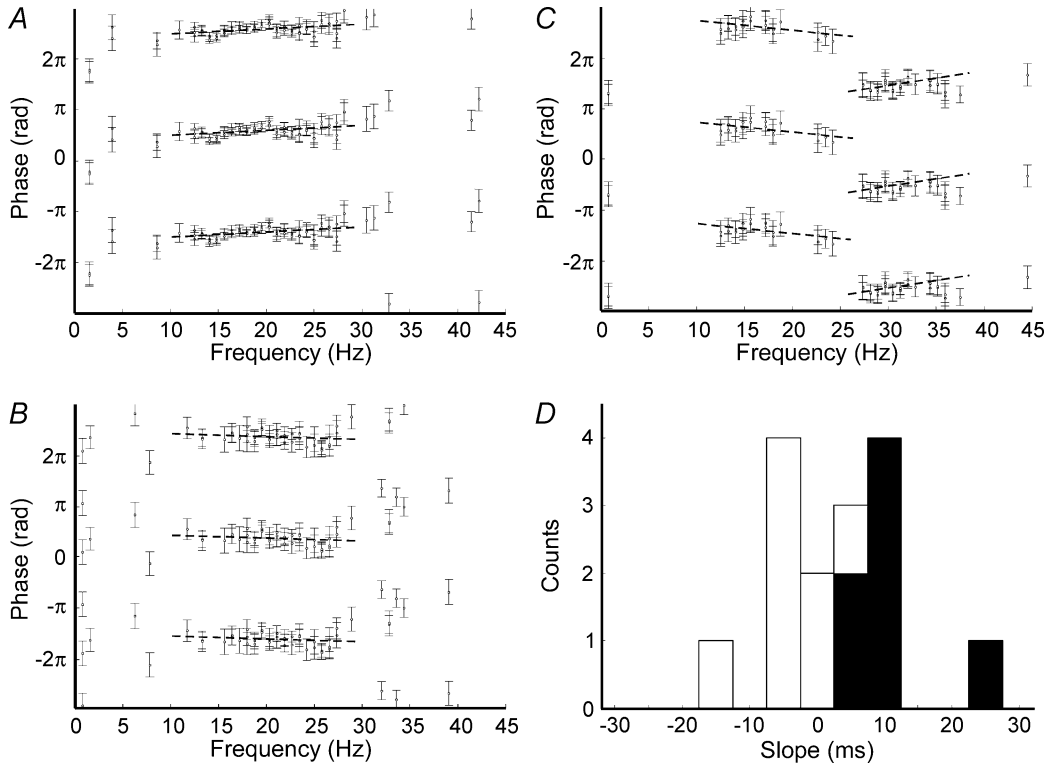

Figure 3. Phase slope grouping method
Plots (*A*–*C*) are single-subject examples of coherence phase *versus* frequency. Phase estimates from each of the three intrinsic hand muscles have been superimposed. Each point is plotted three times at phases separated by 2π radians, to allow linear trends to be visualized across cycle boundaries. Points are only shown for frequencies with significant coherence. Error bars show 95% confidence limits. Broken lines show linear regression fit. *A*, subject 2rd, with a phase–frequency regression slope significantly different from zero. *B*, subject 8cnr with regression slope not significantly different from zero. *C*, subject 2kb showed a zero-slope relationship for low frequencies of coherence, but a significantly non-zero slope at higher frequencies. *D*, histogram of delays between EEG and EMG calculated from regression slopes in all subjects. Positive delays indicate EEG leads EMG. Black bars show slopes significantly different from zero.

more consistent changes were seen in the forearm muscle EMGs. There was generally a shift of power to lower frequencies. Whereas the power spectra of the unrectified EMG in Fig. 2*D* represent mainly the properties of the MUAPs, the power spectra of the rectified EMG depend on both MUAP properties and the extent of oscillatory synchronization in the muscle (Kilner *et al.* 2002). The changes seen in Fig. 5*G–I* probably reflect

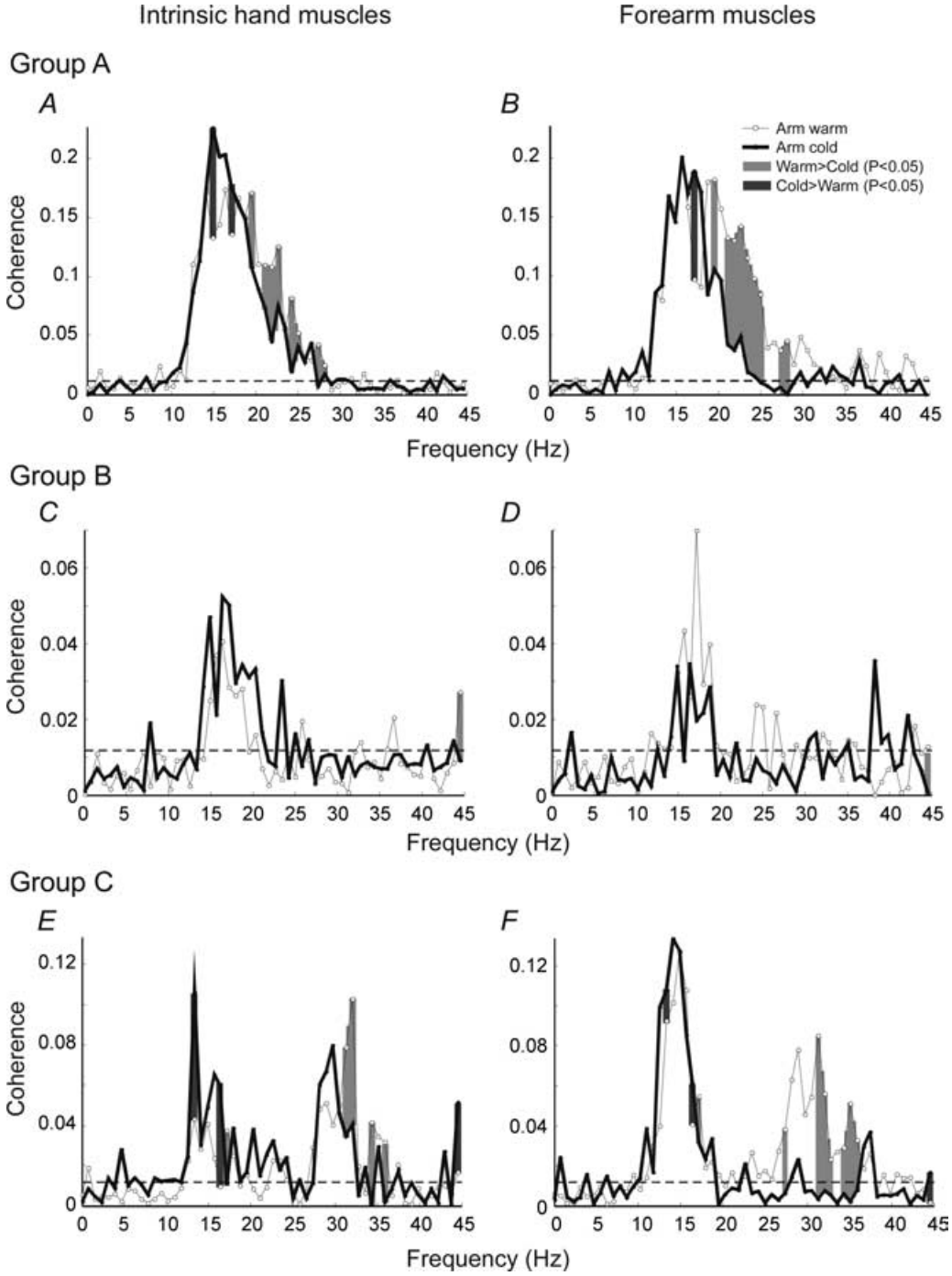

Figure 4. Single-subject examples of coherence changes after cooling
A, *C* and *E*, coherence spectra averaged across the three intrinsic hand muscles recorded; *B*, *D* and *E*, coherence averaged across the two forearm muscles recorded. *A* and *B*, Group A subject 2rd. *C* and *D*, Group B subject 8cnr. *E* and *F*, anomalous subject 2kb, not classified into either group. In all plots, thin lines show control, thick lines show cold data. Grey shading marks bins where control and cold spectra were significantly different ($P < 0.05$). Coherence below the broken line is not significantly different from zero.

mainly the lengthening of MUAP duration revealed by Fig. 2*D*; the non-linear nature of the rectification operation means that there is no straightforward way to predict how the power spectra of the rectified EMG should behave following a change in the spectra of the raw EMG.

Figure 6 illustrates corticomuscular coherence data averaged across all subjects in each group. Spectra have been separately averaged for coherence with intrinsic hand and forearm muscles. Group A showed a broad band of significant coherence from 11.1 Hz to 30.4 Hz in both warm and cold conditions for the intrinsic muscles (Fig. 6*A*). This was similar for the forearm muscles, with the coherent band extending from 11.7 Hz to 38.3 Hz (Fig. 6*B*). In both muscle groups, a robust significant decrease in coherence was observed between ∼20 Hz and 25 Hz after cooling (light grey bars, Fig. 6*A* and *B*). This decrease was of a larger magnitude for the forearm muscles – the peak coherence of 0.097 in the warm condition was at 21.1 Hz for this muscle group, decreasing to 0.035 following cooling, a reduction of 63.9%. By comparison, the peak warm coherence of 0.095 at 21.0 Hz for the intrinsic muscles only decreased by 28.4% to 0.068 after cooling.

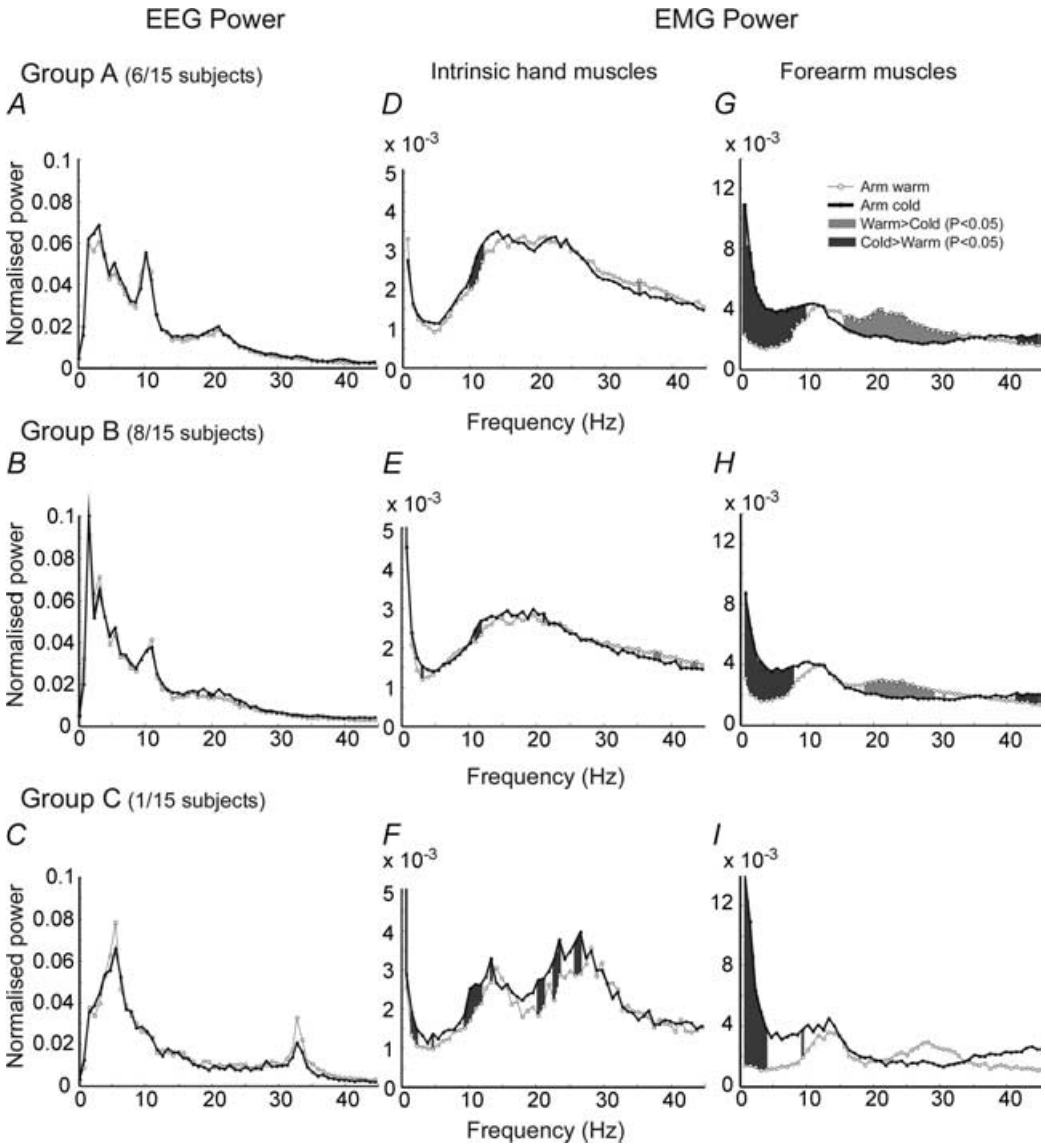

Figure 5. The effect of arm cooling on EEG and EMG power spectra averaged across subjects in each group

A–*C*, EEG power. *D*–*F*, full-wave-rectified EMG power averaged over intrinsic hand muscles. *G*–*I*, full-wave-rectified EMG power averaged over forearm muscles. *A*, *D*, *G*, Group A subjects. *B*, *E*, *H*, Group B subjects. *C*, *F*, *I*, anomalous subject not classified into either group. In all panels, thin line shows control data with arm warm; thick line after cooling. Grey shading marks bins where cooling significantly changes the measure ($P < 0.05$).

The averaged coherence data for Group B subjects showed a number of clear differences. The baseline level of coherence in the warm condition was smaller in both muscle groups than for Group A. For the intrinsic hand muscles, Group B subjects had a peak control coherence of 0.028 at 19.5 Hz, compared to 0.095 (at 21.1 Hz) for Group A. The same pattern was observed for the forearm muscles, with a peak control coherence of 0.034

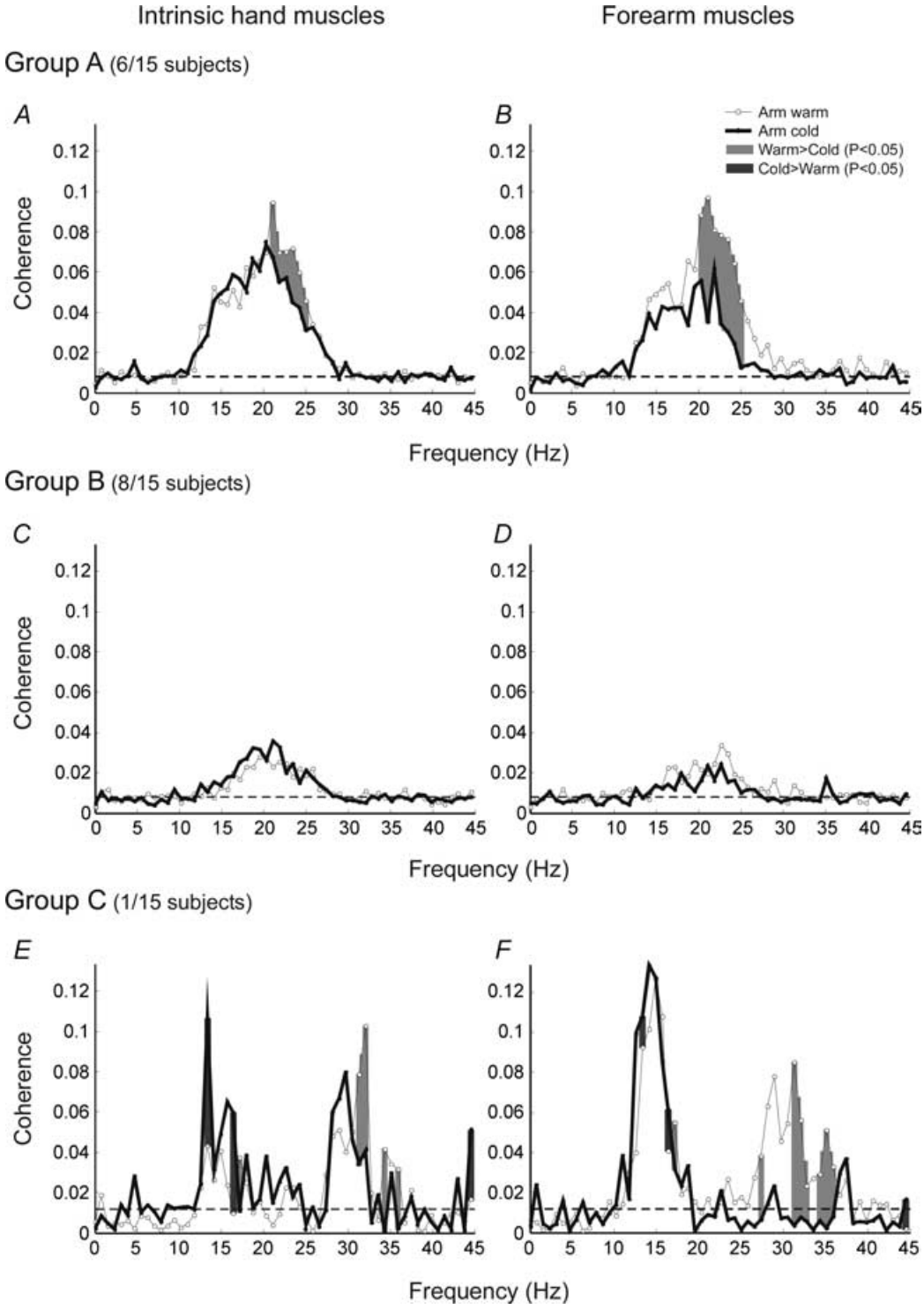

Figure 6. Coherence changes following arm cooling averaged across subjects in each group
A, *C* and *E*, data averaged across intrinsic hand muscles; *B*, *D* and *E*, data averaged across forearm muscles. *A* and *B*, Group A subjects. *C* and *D*, Group B subjects. *E* and *F*, anomalous subject not classified into either group. Same plotting conventions as in Fig. 5. Coherence below the broken line is not significantly different from zero.

(22.6 Hz) seen for Group B compared to 0.097 (21.1 Hz) for Group A. This low Group B coherence did not change significantly after cooling (Fig. 6*C* and *D*). For the intrinsic muscles, the band of significant coherence extended from 12.5 Hz to 28.9 Hz, with a peak warm value of 0.028 at 19.5 Hz (Fig. 6*C*). Following cooling, this value increased to 0.032, a change that was not significant. The same pattern was seen for the forearm muscles (Fig. 6*D*). Figure 6*E* and *F* shows the same analysis for the subject who did not fit into either group; these plots are identical to those shown in Fig. 4*E* and *F*. For the low-frequency range, where this subject's phase–frequency relationship was similar to Group B, there was no significant change in coherence following cooling, as seen in Group B. For the high-frequency band, where the phase–frequency plot behaved as Group A, the coherence was decreased by cooling. The results from this unusual subject are therefore entirely in accordance with the data from the remaining subjects, and provide further confidence that the subdivision of the population has an underlying physiological basis.

Effects of cooling on coherence phase

Given the clear increase in nervous conduction delay produced by cooling, we were interested to determine what effect this had upon the phase–frequency relationship of coherence. On the basis of an 'efferent only' coherence genesis hypothesis, cooling should lead simply to an increase in the phase–frequency slope, equal to the increase in peripheral conduction delay.

Coherence phase was calculated for the intrinsic hand muscles both before and after cooling. The phase for bins with coherence which was significantly non-zero was plotted against frequency, again with superimposition of points from all the intrinsic hand muscles on a single plot. Regression lines were then fitted to the points in the region (or regions for the single subject who did not fit into Group A or B) of strongest coherence, and the gradients determined. For Group A subjects classified as showing a linearly increasing phase–frequency relationship in the control data (Fig. 3*A*), all also had a linear relationship after the arm was cooled; the slope of the regression line was increased. Data from a single subject are illustrated in Fig. 7*A*. Similarly, all but two of the subjects originally classified as Group B, with a flat relationship, retained this pattern after cooling (single-subject example in Fig. 7*B*). Regression slopes fitted to the cold data for these subjects had slopes not significantly different from zero, although in every case the line was shifted vertically upwards after cooling (Fig. 7*B*). The remaining two Group B subjects converted to a Group A pattern after cooling. The anomalous subject again showed changes consistent with both Group A and Group B: the low-frequency points retained their flat phase relationship after cooling, while for the higher-frequency bins there was an increase in the slope of the best fit line (Fig. 7*C*).

If corticomuscular coherence represents a purely efferent phenomenon, then the slope of the line fitted to the coherence phase *versus* frequency plot should give the efferent conduction delay. The change in this slope following arm cooling should then equal the increase in PMCT calculated using the F-wave technique as described in Methods. Figure 7*D* plots the change in delay calculated from the coherence phase of the intrinsic hand muscles *versus* the measured (F-wave) change in PMCT of AbPB after cooling. Each point represents this comparison for a single subject (there are only 14 points because one subject's F-wave data were unavailable for technical reasons). The data were fitted with a regression line constrained to pass through the origin; the slope was 2.33 (95% confidence limits of 1.30–3.36). This analysis included all subjects, not just those from Group A who showed a change in phase–frequency slope after cooling. In order to ensure that the Group B data had not biased the regression analysis, Fig. 7*D* was replotted using only Group A data (figure not shown). The regression slope was similar to the analysis using all subjects, and was calculated as 2.06 (95% confidence limits of 1.26–2.86). A further control was carried out to ensure that the observed small increase in M-wave duration (Fig. 2*C*) was not responsible for the increased phase delay. The regression was again recalculated but with (PMCT change +M-wave duration change) as the abscissa. Once again, the calculated slope was close to 2 (1.84, 95% confidence limits 1.06–2.62). The change in delay estimated from the coherence phase was therefore significantly larger than either the change in PMCT alone, or the change in PMCT plus that in M-wave duration.

Discussion

Coherence phase

Previous reports on the phase of corticomuscular coherence are conflicting. Some authors claim a linearly increasing phase–frequency relationship (Salenius *et al.* 1997; Brown *et al.* 1998; Marsden *et al.* 1999; Mima *et al.* 2000; Gross *et al.* 2000), although they often illustrate subjects with strong coherence. Others show a constant phase relationship across all frequencies (Halliday *et al.* 1998). Where linearly increasing relationships are seen, an attempt is often made to correlate the slope of the best fit line with absolute corticomuscular conduction delays, measured from the latency of an EMG response to transcranial magnetic brain stimulation (TMS) over the primary motor cortex. Most authors claim some agreement, which has been used to support an efferent corticospinal route for corticomuscular coherence. However, this comparison is almost certainly

flawed. Coherence measures the delay between similar parts of an oscillation cycle, whereas latencies measured using TMS are normally taken to the onset of the response. If a valid comparison is to be made, the TMS latency should be measured to the peak of the EMG response. Additionally, TMS will preferentially activate the larger, faster corticomotoneuronal cells, whereas coherence would most likely be mediated by the whole population of corticomotoneuronal cells, including those with slower conduction velocities. For these reasons, it might be expected that the coherence phase–frequency plot would have a slope larger than the onset latency of responses to TMS. However, the reported phase delays are usually smaller than expected (Brown *et al.* 1998; Mima *et al.* 2000).

One important finding of the present study is that corticomuscular coherence does not behave in a uniform way across subjects. This heterogeneity may underlie the conflicting results in the literature. When subjects were separated according to the nature of their phase–frequency regression fits, further differences between the groups emerged. Group A subjects had higher coherence in the control (warm) condition than Group B. They had a marked reduction in coherence following cooling, whereas cooling did not affect the coherence magnitude for Group B. This implies that separation of subjects into two main groups reflected genuine differences, rather than being an artefact of statistical thresholding of the phase–frequency regression slopes. Kilner *et al.* (1999) also found it necessary to divide their subject database into two groups.

There are several possible reasons why corticomuscular coherence might be different in different subjects. It could reflect differences in the way in which subjects process

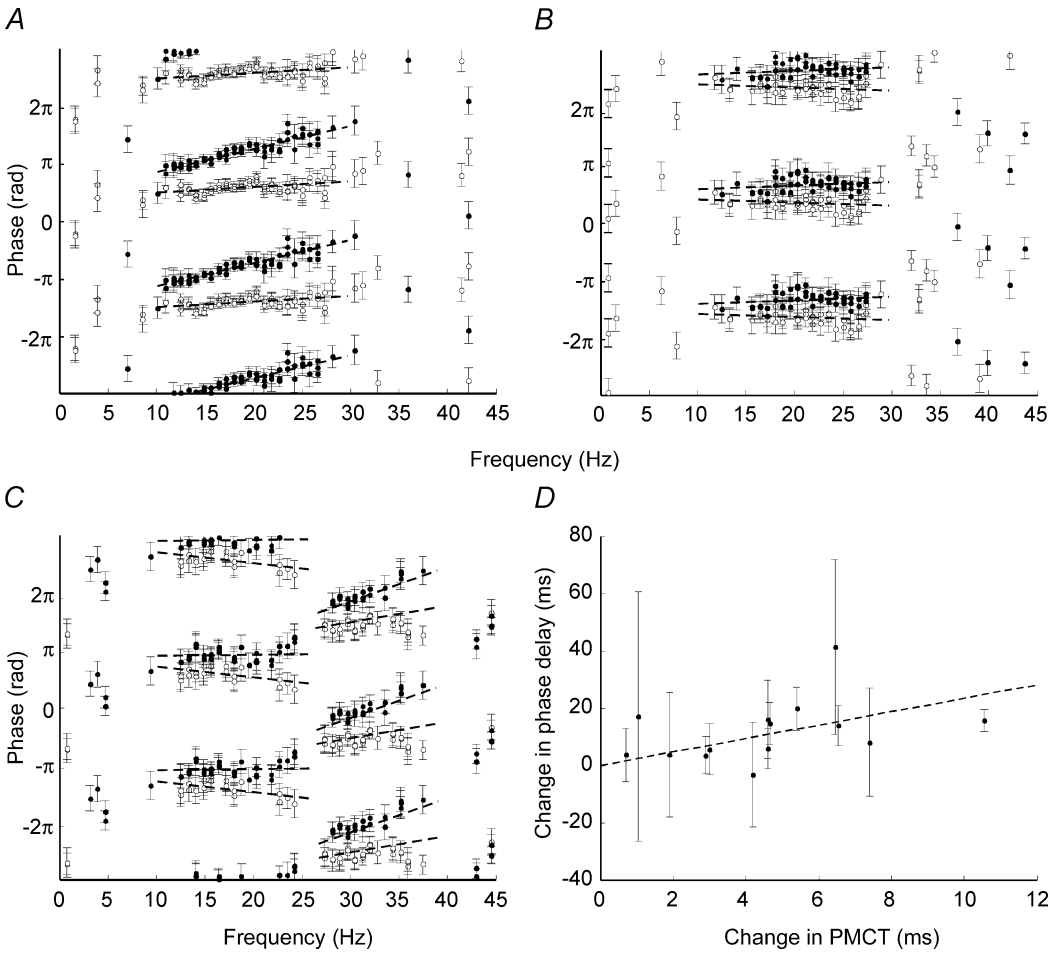

Figure 7. Changes in coherence phase after cooling
A, Group A subject 2rd. *B*, Group B subject 8cnr. *C*, anomalous subject 2kb. Phase plotting conventions as in Fig. 3A–C. ○, control data; ●, after cooling. *D*, change in phase delay plotted *versus* change in peripheral motor conduction time (PMCT) following arm cooling. Phase delay was calculated from the difference in coherence phase–frequency regression slopes using intrinsic hand muscles. PMCT was measured from the AbPB muscle. Each point represents one subject. Error bars show 95% confidence limits, calculated from the confidence limits on the regression slopes. Broken line shows a linear regression fit constrained to intersect the origin.

and use information in the control of their movements; it would be interesting to determine whether Groups A and B exhibit measurable differences in motor performance. Alternatively, the differences could be due to individual variation in the location of the motor cortex relative to the bony landmarks of the skull used to position the electrodes. However, both of these possibilities are rendered less likely by the fact that a single subject can simultaneously show both Group A and Group B characteristics over different frequency ranges.

A more plausible explanation may be that corticomuscular coherence in all subjects results from multiple interacting oscillatory processes, each with different underlying phase relationships. The relative extent to which these contribute to the measured coherence could depend on many variables, such as electrode location and oscillation frequency. This could lead not only to interindividual variability, but also to intraindividual variation across the frequency range investigated.

Change in coherence phase following arm cooling

The population scatter plot of Fig. 7*D* indicated that the change in phase–frequency slope following cooling was on average more than twice that expected from the measured change in efferent conduction time. Although the motor unit action potential durations in the intrinsic hand muscles were slightly affected by the cooling protocol (Fig. 2*C* and *D*), the change in phase–frequency slope was still significantly larger even than the sum of the increases in PMCT and M-wave duration. On its own, this is good evidence against a purely efferent pathway for corticomuscular coherence. It is additionally of interest that the change in slope was approximately twice the efferent slowing. The large-diameter afferent fibres have similar conduction velocities to the efferents (Clough *et al.* 1968; Cheney & Preston, 1976), and cooling therefore probably slows their conduction by a comparable amount to that measured for the motor fibres. The increase in the total afferent–efferent feedback loop delay would therefore, on average, match well with the increased slope of the phase–frequency relationship.

Change in coherence following arm cooling

The separation of subjects into two distinct population groups was supported by the different effect of arm cooling on the size of corticomuscular coherence in these groups. However, the changes do not fit with any straightforward model of coherence genesis. Data from the Group A subjects, where the coherence phase showed a linearly increasing relationship with frequency, fit most closely with generation of coherence via efferent pathways introducing fixed delays. However, in these subjects the magnitude of coherence was markedly reduced following cooling. Yet if all that has changed is the conduction delay, only the phase, and not the coherence magnitude should change. By contrast, the Group B subjects showed a phase–frequency profile which could not be interpreted as simple efferent conduction of oscillations. However, the coherence magnitude was unchanged by cooling, despite these subjects demonstrating comparable slowing of conduction as assessed by F-waves. The veracity of these findings was confirmed by the data from the single anomalous subject. Over the low-frequency range, where coherence phase did not depend on frequency, the coherence magnitude was unaffected by cooling in this person. At higher frequencies, where phase increased linearly with frequency, cooling reduced coherence.

Two other recently published studies were able to show a reduction in oscillatory coupling in the motor system using different but related methods of altering peripheral nervous conduction. Pohja & Salenius (2003) measured corticomuscular coherence before and after partial deafferentation of the arm by ischaemic block, which demonstratively slowed nervous conduction. Measurements were made prior to complete block of the efferent fibres; however, at this stage some block of afferent systems is likely (Cody *et al.* 1987; Baker & Matthews, 1993). On average, corticomuscular coherence was reduced following ischaemia, although the illustrated single-subject data show considerable variability, and it is possible that the subjects could also be subdivided into two groups as here.

Fisher *et al.* (2002) blocked the cutaneous afferents from the index finger and thumb using local anaesthetic, and measured the effect on coherence between hand muscle EMG recordings. Such intermuscle synchrony is likely to be generated by common oscillatory inputs from the cortex (Datta *et al.* 1991; Farmer *et al.* 1993). In eight out of ten subjects, coherence was significant in the control condition, and was reduced following anaesthesia. The two remaining subjects had low initial coherence, and there was no change after anaesthesia. These results are again similar to our own.

Implications for generation of corticomuscular coherence

It is most likely, as postulated above, that the coherence which we can observe experimentally is a complex composite of multiple interacting processes, probably with a contribution from both afferent and efferent systems. For example, it is known that the monosynaptic stretch reflex arc can generate oscillations, or tremor, with a period of twice the loop delay (Lippold, 1970; Brown *et al.* 1982). When such a loop is driven with oscillatory descending inputs, we speculate that there will be resonance or cancellation, depending on the frequency. Coherence would then represent the interaction between oscillatory descending inputs and the intrinsic tendency to oscillate of

the peripheral reflex loop. Changing the loop delay could alter corticomuscular coherence by shifting the frequencies at which interactions with reflex loops occur. The total reflex loop time includes the time for the muscle to generate force; this was greatly increased by cooling for the forearm muscles, whereas the changes for the intrinsic muscles were less marked (Fig. 2*A* and *B*). Interestingly, the changes in coherence following cooling in Group A subjects were greater for the forearm muscles than the intrinsic hand muscles, which might be expected if the reflex loop time was the key variable, rather than solely efferent or afferent nervous conduction delay.

These findings are of significant importance in the understanding and development of corticomuscular coherence as a clinical and experimental tool, as well as in further exploring its role in the human motor system. We have recently demonstrated two situations in which coherence can be dissociated from the power of sensorimotor cortical oscillations, suggesting that it is an independent variable of significance as an entity in itself (Baker & Baker, 2003; Riddle *et al.*, 2004). An involvement of afferent systems in the genesis of coherence would point towards a role in sensorimotor integration within the motor system, perhaps aiding in the performance of skilled motor tasks or the global control of, for example, hand movement.

References

Baker MR & Baker SN (2003). The effect of diazepam on motor cortical oscillations and corticomuscular coherence studied in man. *J Physiol* **546**, 931–942.

Baker SN & Matthews HR (1993). Differential effect of ischaemia on the reflex electromyographic responses to stretch and electrical stimulation in the human first dorsal interosseous muscle. *J Physiol* **459**, 456P.

Baker SN, Olivier E & Lemon RN (1997). Coherent oscillations in monkey motor cortex and hand muscle EMG show task dependent modulation. *J Physiol* **501**, 225–241.

Baker SN, Pinches EM & Lemon SN (2003). Synchronisation in monkey motor cortex during a precision grip task. II. Effect of oscillatory activity on corticospinal output. *J Neurophysiol* **89**, 1941–1953.

Brown TI, Rack PM & Ross HF (1982). Different types of tremor in the human thumb. *J Physiol* **332**, 113–123.

Brown P, Salenius S, Rothwell JC & Hari R (1998). Cortical correlate of the Piper rhythm in humans. *J Neurophysiol* **80**, 2911–2917.

Cheney PD & Preston JB (1976). Classification and response characteristics of muscle spindle afferents in the primate. *J Neurophysiol* **39**, 1–8.

Clough JFM, Kernell D & Phillips CG (1968). The distribution of monosynaptic excitation from the pyramidal tract and from primary spindle afferents to motoneurones of the baboon's hand and forearm. *J Physiol* **198**, 145–166.

Cody FW, Goodwin CN & Richardson HC (1987). Effects of ischaemia upon reflex electromyographic responses evoked by stretch and vibration in human wrist flexor muscles. *J Physiol* **391**, 589–609.

Conway BA, Halliday DM, Farmer SF, Shahani U, Maas P, Weir AL & Rosenberg JR (1995). Synchronization between motor cortex and spinal motoneuronal pool during the performance of a maintained motor task in man. *J Physiol* **489**, 917–924.

Datta AK, Farmer SF & Stephens JA (1991). Central nervous pathways underlying synchronization of human motor unit firing studied during voluntary contractions. *J Physiol* **432**, 401–425.

Donoghue JP, Sanes JN, Hatsopoulos NG & Gaal G (1998). Neural discharge and local field potential oscillations in primate motor cortex during voluntary movements. *J Neurophysiol* **79**, 159–173.

Evans CMB & Baker SN (2003). Task dependent inter-manual coupling of 10-Hz discontinuities during slow finger movements. *Eur J Neurosci* **18**, 453–456.

Farmer SF, Bremner FD, Halliday DM, Rosenberg JR & Stephens JA (1993). The frequency content of common synaptic inputs to motoneurones studied during voluntary isometric contraction in man. *J Physiol* **470**, 127–155.

Fisher RJ, Galea MP, Brown P & Lemon RN (2002). Digital nerve anaesthesia decreases EMG-EMG coherence in a human precision grip task. *Exp Brain Res* **145**, 204–214.

Gross J, Tass PA, Salenius S, Hari R, Freund HJ & Schnitzler A (2000). Cortico-muscular synchronization during isometric muscle contraction in humans as revealed by magnetoencephalography. *J Physiol* **527**, 623–631.

Halliday DM, Conway BA, Farmer SF & Rosenberg JR (1998). Using electroencephalography to study functional coupling between cortical activity and electromyograms during voluntary contractions in humans. *Neurosci Lett* **241**, 5–8.

Hari R & Salenius S (1999). Rhythmical corticomuscular communication. *Neuroreport* **10**, 1–10.

Kimura J (1989). *Electrodiagnosis in diseases of muscle and nerve*. FA Davies, Philadelphia.

Kilner JM, Baker SN, Salenius S, Hari R & Lemon RN (2000). Human cortical muscle coherence is directly related to specific motor parameters. *J Neurosci* **20**, 8838–8845.

Kilner JM, Baker SN, Salenius S, Jousmäki V, Hari R & Lemon RN (1999). Task-dependent modulation of 20–30 Hz coherence between rectified EMGs from human hand and forearm muscles. *J Physiol* **516**, 559–570.

Kilner JM, Baker SN & Lemon RN (2002). A novel algorithm to remove electrical cross-talk between surface EMG recordings and its application to the measurement of short-term synchronisation in humans. *J Physiol* **538**, 919–930.

Lemon RN (1979). Thalamic pathway for rapid afferent input from hand to motor cortex in the monkey [proceedings]. *J Physiol* **292**, 55P–56P.

Lippold OC (1970). Oscillation in the stretch reflex arc and the origin of the rhythmical, 8–12 C-S component of physiological tremor. *J Physiol* **206**, 359–382.

McAuley JH, Rothwell JC & Marsden CD (1997). Frequency peaks of tremor, muscle vibration and electromyographic activity at 10 Hz and 40 Hz during human finger muscle contraction may reflect rhythmicites of central neural firing. *Exp Brain Res* **114**, 525–541.

Marsden JF, Farmer SF, Halliday DM, Rosenberg JR & Brown P (1999). The unilateral and bilateral control of motor unit pairs in the first dorsal interosseous and paraspinal muscles in man. *J Physiol* **521**, 553–564.

Matthews PBC (1972). *Mammalian Muscle Receptors and their Central Actions*. E Arnold, London.

Matthews PB (1989). Long-latency stretch reflexes of two intrinsic muscles of the human hand analysed by cooling the arm. *J Physiol* **419**, 519–538.

Mima T & Hallett M (1999). Electroencephalographic analysis of cortico-muscular coherence: reference effect, volume conduction and generator mechanism. *Clin Neurophysiol* **110**, 1892–1899.

Mima T, Steger J, Schulman AE, Gerloff C & Hallett M (2000). Electroencephalographic measurement of motor cortex control of muscle activity in humans. *Clin Neurophysiol* **111**, 326–337.

Murthy VN & Fetz EE (1996). Oscillatory activity in sensorimotor cortex of awake monkeys: synchronization of local field potentials and relation to behavior. *J Neurophysiol* **76**, 3949–3967.

Olivier E, Baker SN & Lemon RN (2002). Comparison of direcct and indirect measurements of the central motor conduction time in the monkey. *Clin Neurophysiol* **113**, 469–477.

Pfurtscheller G & Neuper C (1992). Simultaneous EEG 10 Hz desynchronization and 40 Hz synchronization during finger movements. *Neuroreport* **3**, 1057–1060.

Pfurtscheller G, Stancak A & Neuper C (1996). Post-movement beta synchronization. A correlate of an idling motor area? *Electroencephalogr Clin Neurophysiol* **98**, 281–293.

Pohja M & Salenius S (2003). Modulation of cortex-muscle oscillatory interaction by ischaemia-induced deafferentation? *Neuroreport* **14**, 321–324.

Riddle CN, Baker MR & Baker SN (2004). The effect of carbamazepine on human corticomuscular coherence. *Neuroimage* **22**, 333–340.

Rosenberg JR, Amjad AM, Breeze P, Brillinger DR & Halliday DM (1989). The fourier approach to the identification of functional coupling between neuronal spike trains. *Prog Biophys Mol Biol* **53**, 1–31.

Salenius S, Portin K, Kajola M, Salmelin R & Hari R (1997). Cortical control of human motoneuron firing during isometric contraction. *J Neurophysiol* **77**, 3401–3405.

Salmelin R & Hari R (1994). Spatiotemporal characteristics of sensorimotor neuromagnetic rhythms related to thumb movement. *Neuroscience* **60**, 537–550.

Stancak A & Pfurtscheller G (1996). Mu-rhythm changes in brisk and slow self-paced finger movements. *Neuroreport* **7**, 1161–1164.

Stiles RN & Randall JE (1967). Mechanical factors in human tremor frequency. *J Appl Physiol* **23**, 324–330.

Vaillancourt DE & Newell KM (2000). Amplitude changes in the 8–12, 20–25, and 40 Hz oscillations in finger tremor. *Clin Neurophysiol* **111**, 1792–1801.

Acknowledgements

The authors wish to thank the volunteer subjects who gave their time to this study. Funded by The Wellcome Trust.